J MATER SCI 41 (2006) 1757–1768

Porosity dependence of mechanical properties of solid materials

SHAOCHENG JI*, QI GU
Département des Génies Civil, Géologique et des Mines, École Polytechnique de Montréal, Montréal, H3C 3A7, Canada
E-mail: sji@polymtl.ca

BIN XIA
Laboratory of Marginal Sea Geology, Guangzhou Institute of Geochemistry, Chinese Academy of Sciences, Wushan, Guangzhou, 510640, China

Published online: 17 February 2006

The generalized means are used as a simple but elegant mixture rule for providing a unified description of the physical properties of polyphase composites in terms of component properties, volume fractions, and microstructures. This formula is named as the generalized mixture rule (GMR). Taking porous materials as a special class of two-phase composites in which pores are dispersed within a solid framework, the GMR yields a rigorous expression for the porosity dependence of the mechanical properties. Although the GMR is purely mathematical in origin, its connection to the existing theories and its consistence with extensive experimental data suggests that it should have some physical validity as a hypothesis or at least a very handy tool for a general description of the mechanical properties of multiphase materials including porous solids.

1. Introduction

Porosity is an important microstructural feature in most natural and man-made materials and often affects significantly physical properties of these materials such as fluid permeability, thermal conductivity, electrical conductivity, dielectric constant, magnetic permeability, diffusion coefficient, acoustic wave velocities, elastic moduli, and yield, rupture or ductile strength. Typical examples of natural porous materials are sediments (e.g., soils, sands and sandstone). Better knowledge about the porosity-dependence of rock mechanical properties is required to anticipate and minimise the technical problems in oil reservoirs such as earth surface subsidence and well-bore instability. Biological materials such as woods and bones are equally porous materials. Man-made porous materials such as foamed metals, sintered ceramics, hollow concretes and cellular polymers are widely used for thermal and acoustic insulation, impact energy absorption, vibration suppression, air or water filtration, fluid flow control, self-lubricating bearing, floatation and lightweight components. Further, traditional construction materials such as bricks, tiles, cements and concretes all are porous. Thus, to model accurately the mechanical properties of candidate solid materials in terms of their component properties, porosity and microstructure has broad significance for a wide range of fields from materials engineering to Earth sciences.

The modeling of composite mechanical properties is involved in the utilization of appropriate mixture rules. Actually some of the important rules can be unified by a generalized mixture rule (GMR) expressed as:

$$M_c^J = \sum_{i=1}^{N} \left(V_i M_i^J \right) \tag{1}$$

where M is a specific property (e.g., Young's modulus, yield strength or ductile flow strength). V is the volume fraction of component, the subscripts i and c represent, respectively, the ith phase and the composite consisting of N phases,

$$\sum_{i=1}^{N} V_i = 1 \tag{2}$$

Effects of microstructures are expressed by a scaling, fractal parameter J, which is mainly controlled by the

*Author to whom all correspondence should be addressed.
0022-2461
DOI: 10.1007/s10853-006-2871-9

shape, size distribution, and distribution (continuity and connectivity) of the phases [1, 2]. $M_c(J)$ has the following characteristics:

(a) $M_c(J)$ is a continuous, monotone increasing function for all J values in the ranges $(-\infty \leq J \leq \infty)$. This monotonicity stands with respect to either the volume fractions or the physical properties.

(b) For $J < 1, J = 1$ and $J > 1, M_c(J)$ as a function of the individual grades of membership M_i is strongly concave, linear, and strongly convex, respectively.

(c) For a binary system that consists of a strong phase (s) and a weak phase (w), $J < 0$ for the weak-phase supported structure while $J > 0$ for the strong-phase supported structure [1, 2]. The GMR fulfills the following boundary conditions: for $V_s = 0$ (pure weak phase aggregate), the effective properties are equivalent to the properties of the weak phase for all values of J. Similarly, for $V_s = 1$ (pure strong phase aggregate), the effective properties are equivalent to the properties of the strong phase for all values of J. In the circumstance that $M_s = M_w$ (two phases have an equivalent property), then $M_c = M_s = M_w$ for all values of J and all values of V_s.

(d) The case $J = 1$ yields the arithmetic mean or Voigt average (which assumes constant strain). The case $J = -1$ yields the harmonic mean or Reuss average (which assumes constant stress). For isotropic composites, the Voigt and Reuss averages are generally regarded as the upper and lower bounds for effective elastic properties [3]. For a composite consisting of rigid particles in a steady-state flowing matrix, however, its effective creep strength may be lower than the Reuss bound as long as the stress exponent of the matrix is sufficiently large, say, >4. The GMR with $J \to 0$ yields the geometrical mean. The latter becomes physically meaningless when one of the constituent phases has a null property. In this special case, the overall property of the composite acquired from the geometrical mean will always vanish regardless of the volume fraction of the constituent that has a null property.

Recently, Ji [2] showed that various celebrated expressions such as Einstein's equation for ideal, dilute suspensions [4] and Roscoe's formula for general solid-liquid suspensions [5] can be derived as special cases from the GMR using the microstructural parameter $J = -0.4$. It has been demonstrated that the GMR works well for describing various mechanical properties (e.g., elastic moduli, hardness, yield, and flow strengths for wide ranges of multiphase systems from natural rocks to industrial ceramics and alloys. In this paper, we will display that the GMR is also a good descriptive model to fit the experimental data for the elastic and plastic mechanical properties of porous materials (i.e., $M_s/M_w \to \infty$).

2. Analysis

For a two-phase composite, Equation 1 can be simplified:

$$M_c^J = (1 - V_w)M_s^J + V_w M_w^J \tag{3}$$

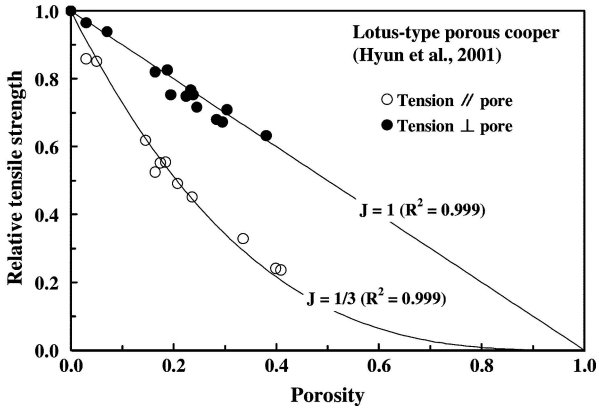

Figure 1 Relative tensile strengths of lotus-type porous cooper [6] as a function of porosity. Theoretical curves labelled according to J values.

Porous materials are considered as a special class of two-phase composites in which null strength pores are dispersed within a solid framework. Then setting the mechanical property of the weak phase equals to zero (i.e., $M_w = 0$) and taking V_w as the volume fraction porosity (p) allow an estimation of the effect of porosity on the property. Equation 3 can be written as

$$\frac{M_c}{M_s} = (1 - p)^{1/J} = V_s^{1/J} = \left(\frac{\rho_c}{\rho_s}\right)^{1/J} \tag{4}$$

where J is the parameter that depends on the geometrical shape, spatial arrangement, orientation and size distribution of pores, and in turn on the materials and the fabrication method (i.e., cold pressing, sintering, or hot isostatic pressing), ρ_c and ρ_s are the densities of the porous and nonporous materials, respectively. ρ_c/ρ_s is the relative density that equals the volume fraction mass. On the plots of $\log(M_c/M_s)$ versus $\log(1 - p)$ or $\log(\rho_c/\rho_s)$, $1/J$ is the slope of the property dependence over the linear range. The value of J should lie in the range from 0 to 1, giving a wide range of properties at a given relative density or porosity. The variation of J with microstructure yields a large possibility to optimize the mechanical properties of porous solids. Further, porosity has a greater effect on the mechanical properties at smaller values of J.

$J = 1$ for porous materials with long cylindrical or hexagonal pores aligned parallel to the stress direction,

$$\frac{M_c}{M_s} = 1 - p = \frac{\rho_c}{\rho_s} \tag{5}$$

Equation 5 yields a linear relationship between M_c/M_s and p, and good agreement with experimental results of lotus-type porous metals with the long pores parallel to the loading direction [6, 7] (see Fig. 1). $J = 0$ represents an extreme case where the effective property of a porous material will vanish, regardless of porosity. Generally, intergranular, continuous, channel pores cavities cause a lower J value than intragranular, isolated and rounded pores. The open pores exhibit a lower J value and thus more

pronounced effects on the effective mechanical properties than the closed pores. Thus, the complex dependence of J on microstructure is a crucial subject for study in order to better predict and optimize the mechanical properties of porous solids.

Equation 4 can be expanded to a power series:

$$\frac{M_c}{M_s} = 1 + \left(-\frac{1}{J}p\right) + \frac{\frac{1}{J}\left(\frac{1}{J}-1\right)}{2}p^2 + \frac{\left(-\frac{1}{J}\right)\left(\frac{1}{J}-1\right)\left(\frac{1}{J}-2\right)}{6}p^3 + \cdots \quad (6)$$

For low values of porosity ($p \ll 1$), Equation 6 can be reasonably approximated by

$$\frac{M_c}{M_s} = 1 - \frac{1}{J}p \quad (7)$$

Equation 7 indicates a linear relation between M_c/M_s and p at low porosities ($p < 0.10$–0.15).

The pore shape, which is one of the most important factors to affect the J value, can be characterized by the shape factor (S) that is defined below:

$$S = 4\pi A/L^2 \quad (8)$$

where A is the pore area and L is the pore perimeter in a random thin section. Both A and L can be measured using quantitative image analysis. S decreases in magnitude as the pore outline becomes more irregular. For example, $S = 1$ for a perfect circle, $S = 0.785$ for a square, $S = 0.604$ for equilateral triangle, and S approaches zero if the pore shape becomes a line [8]. It is found that spherical pores generally occur at low porosities. As the porosity increases, the shape factor decreases and the pore geometry becomes increasingly more complex. When the porosity is higher than a critical value (p_{c1}), the pores become increasingly more open [9]. Moreover, large pores are generally more irregular than small pores, indicating that the large pores may form from the agglomeration of small pores. As a result, the S value decreases [10] and so does the J value with increasing pore size. Conversely, a trend of decreasing S with decreasing pore size may result if small irregular pores were produced by fragmentation of large smooth ones. Thus, the J value may reflect the formation processes of the materials.

Furthermore, the mechanical properties of a nonporous material can be estimated from its porous counterpart according to the following equation:

$$M_s = \left[\frac{M_c^J}{1-\phi}\right]^{1/J} \quad (9)$$

For an inversion purpose, an analytical formula like Equation 9 is advantageous than complicated and tedious computational codes.

3. Comparison with other expressions

Because it is obviously prohibitive to determine experimentally the effective properties of each porous material of interest, numerous empirical and theoretical relations have been proposed to describe the dependence of mechanical property of materials to their porosities. The empirical relations attempt to best-fit experimental data, but the physical meaning of the relations is unclear. However, the theoretical models, in spite of using the first physical principles, are based on some idealized microstructures (e.g., uniform spherical, cylindrical or cubic pores are arranged in a cubic array [11–14], and the derived correlations between the effective properties and porosity often cannot be extended to real materials with irregular shapes, nonuniform size and random distribution of pores.

One of the most popular expressions is the following:

$$\frac{M_c}{M_s} = (1-p)^m \quad (10)$$

where m is an adjustable parameter. In Equation 10, M represents the Young's modulus (E), shear modulus (G), bulk modulus (K), yield strength (σ_y), rupture strength (σ_r), or flow strength (σ_f). Equation 10 was first proposed by Balshin [15] as an empirical equation. Based on the assumption that a porous material consists of a 3D intertwined, continuous network of material chains and open-pore channels, Wong *et al.* [16] and Wagh *et al.* [17] derived Equation 10 as a theoretical formula for the porosity dependence of the Young's modulus. These authors named the expression as the connected-grain or open pore model.

The comparison of Equation 10 with Equation 4 yields $m = 1/J$. In the elastic field, the exponent m has been related to the stress concentrations that develop around pores [18, 19], and named as the elastic stress concentration factor of the pores [7, 20–22]. Based on 3D elasticity theory for the stress concentration around spheroidal pores (Z is the axis of revolution and X is the axis perpendicular to Z) in a material under uniaxial stress, Boccaccini *et al.* [21] obtained the following results: For spherical pores (Z/X = 1), $m = 2$ and thus $J = 0.5$. For infinitely long cylindrical pores (Z/X$\rightarrow\infty$) oriented perpendicular to the stress direction, $m = 3$ and thus $J = 1/3$ (Fig. 1). For lotus-type porous materials with long cylindrical or hexagonal pores (Z/X$\rightarrow\infty$) oriented parallel to the stress direction, there is no stress concentration effect [23] and $m\rightarrow 1$ or $J\rightarrow 1$ (Fig. 1).

The porosity dependence of physical properties of porous materials can be evaluated using an assumption that the relative property of interest (M_c/M_s) is equal to the ratio of the minimum solid area (MSA) to the cell area normal to the reference stress [14]. The MSA can be easily calculated for idealized structures, that is, regular stacking of uniform (spherical, spheroidal, cylindrical or cubic) pores in a continuous solid medium [11, 12]. The variations of the MSA with porosity have been studied for various ordered arrays of pores. It is generally found

that the MSA can be related to the porosity for relatively low volume fraction of porosity ($p \leq \sim 0.4 p_c$, where p_c is the critical porosity that corresponds to the percolation limit of the solid phase) by an exponential function [14, 24, 25]:

$$\frac{A}{A_0} = \exp(-bp) \tag{11}$$

where A and A_0 are, respectively, the solid areas of porous and porosity-free materials, normal to the reference direction; and b is a constant that depends on the array of pores in the material. In other words, the value of $\ln(A/A_0)$ decreases linearly with the porosity with b equal to the slope.

As the relative value of M_c/M_s is directly proportional to that of A/A_0 [14], thus:

$$\frac{M_c}{M_s} = \exp(-bp) \tag{12}$$

Equation 12 was proposed first by Duckworth [26] as an empirical equation and since then it has been widely used to predict the effective mechanical properties of porous materials with reasonable accuracy [14, 24, 25, 27]. According to Ramakrishan and Arunachalam [28], Equation 12 can be obtained using the differential methods [29–31] under certain approximations.

Unlike Equation 4, Equation 12 displays an evident disadvantage: the boundary condition that M_c should be equal to zero when p is equal to 1 is not satisfied [32]. Actually Equation 12 breaks down when $p \rightarrow p_c$. Consequently, Equation 12 is not valid over the full range of porosity from 0 to 1 and can be used for only low values of porosity (i.e., $p \leq 0.30$).

Equation 12 can be expanded to a power series:

$$\frac{M_c}{M_s} = 1 + (-bp) + \frac{(-bp)^2}{2} + \frac{(-bp)^3}{6} + \cdots \tag{13}$$

For low values of porosity (i.e., $p \ll 1$), Equation 13 can be reasonably approximated by the first term of the above series expansion.

$$\frac{M_c}{M_s} = 1 - bp \tag{14}$$

Equation 14 yields the same formula as that proposed by Hashin [33] and Rossi [34].

Comparison between Equations 7 and 14 gives $J = 1/b$. For many porous polycrystalline materials, the b values have been determined for each property and can be converted to the J values (Fig. 2). Therefore, the exponential expression as described by Equation 12 can be derived directly from the GMR for the porous materials with relatively low values of porosity ($p \ll 1$ where there are most data).

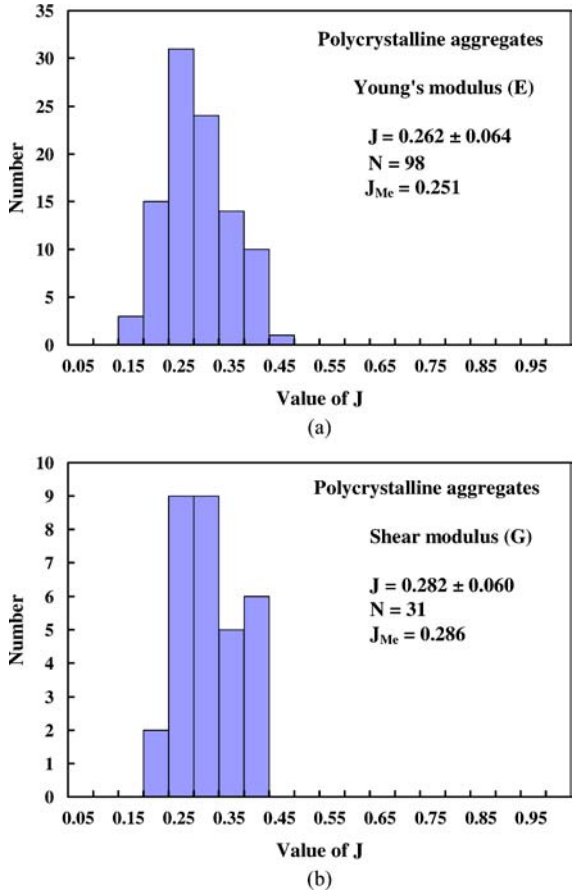

Figure 2 Histograms of J-values for the Young's modulus (a) and shear modulus (b) of polycrystalline aggregates. Data mainly from [14, 25]. N, the number of measurements; J_{Me}, the median (the fiftieth percentile in the distribution).

Considering the linear-elastic edge deflection of open-cell foams, Gibson and Ashby [13] pursued a simple relation for the Young's modulus of the cellular solids:

$$\frac{E_c}{E_s} = C\left(\frac{\rho_c}{\rho_s}\right)^n = C(1-p)^n \tag{15}$$

where C and n are constants that depend on the microstructure of the foam. Setting ρ_c equal to ρ_s or $p = 0$ in Equation 15 does not yield the boundary condition that E_c is equal to E_s if $C \neq 1$. To satisfy this boundary condition will require $C=1$ and in turn Equation 15 becomes identical to our Equation 4 with $J = 1/n$. Fitting the experimental data [35–37] with Equation 15, Gibson and Ashby [13] obtained $n = 2$, which corresponds $J = 0.5$ in Equation 4. In the case of porous materials with a honeycomb structure, Gibson and Ashby [13] show that $n = 1$ (*i.e.*, $J = 1$) and $n = 3$ ($J = 1/3$) for the directions parallel to and perpendicular to the direction of pores, respectively (Fig. 1).

Based on an assumption that the relative property of interest (M_c/M_s) equals the ratio of the minimum solid area (MSA) to the cell area normal to the reference stress, and using an ideal microstructure that uniform spherical

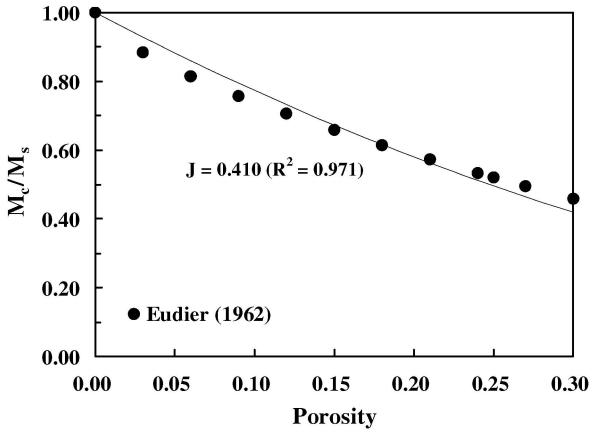

(a)

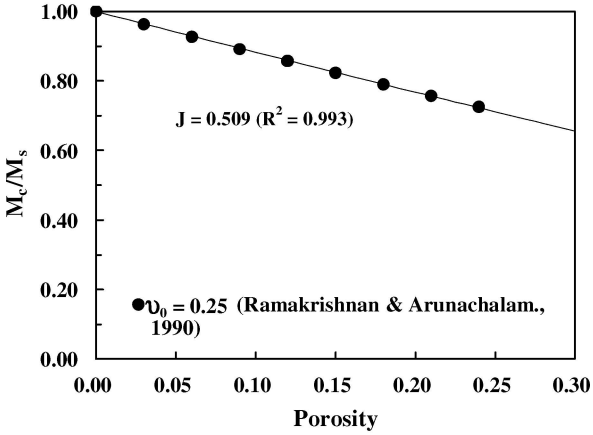

(b)

Figure 3 Comparison of the GMR with the theoretical models of Eudier [11] and Ramakrishnan and Arunachalam [38].

pores are arranged in a simple cubic array, Eudier [11] obtained

$$\frac{M_c}{M_s} = 1 - \pi\left(\frac{3}{4\pi}\right)^{2/3} p^{2/3} = 1 - 1.21p^{2/3} \quad (16)$$

In the Eudier's model, the critical value of p for the cubic packing geometry is $\pi/6$ or 0.524, over which the pores should overlap each other. In other words, a transition from isolated and closed to open and interconnected porous structures occurs when $p \geq 0.524$. Moreover, M_c/M_s will reach zero once $p = 4/(3\sqrt{\pi})$ or 0.752. For $p > P_c = 0.752$, Equation 16 becomes no longer valid. At $p \leq 0.30$, the Eudier's model can be approximated by the GMR with $J = 0.410$ (Fig. 3a).

Further, Ramakrishnan and Arunachalam [38] derived the following equation for an isolated spherical pore geometry:

$$\frac{M_c}{M_s} = \frac{(1-p^2)}{1+\beta p} \quad (17)$$

where β is a parameter that is a function of zero-porosity Poisson's ratio (υ_0) of the solid matrix.

$$\beta_K = \frac{1+\upsilon_0}{2(1-2\upsilon_0)} \quad (18)$$

$$\beta_G = \frac{11-19\upsilon_0}{4(1+\upsilon_0)} \quad (19)$$

$$\beta_E = 2 - 3\upsilon_0 \quad (20)$$

for the bulk (K), shear (G) and Young's (E) moduli, respectively. $\beta_K = \beta_G = \beta_E = 1.25$ when $\upsilon_0 = 0.25$. Equation 17 can be represented by the GMR. For example, the case of $\beta = 1.25$ is approximately equivalent to $J = 0.509$ (Fig. 3b).

For solids containing cubic pores,

$$\frac{M_c}{M_s} = 1 - kp^{2/3} \quad (21)$$

where $k = 1$, $\sqrt{2}$ and $\sqrt{3}$ for cubic pores with their ⟨100⟩, ⟨110⟩ and ⟨111⟩ directions parallel to the reference direction, respectively [14, 39]. Equation 21 with $k = 1$, $\sqrt{2}$ and $\sqrt{3}$ can be approximated, respectively, by the GMR with $J = 0.507$, 0.321 and 0.237 at $p \leq 0.26$ (Fig. 4). Clearly, the J value decreases progressively as the cubic pores are oriented with their ⟨100⟩, ⟨110⟩ and ⟨111⟩ directions parallel to the reference direction.

It is necessary to point out that the theoretical models summarized above, which were based on specific structures, cannot be extended to more general materials with irregular shapes, varied size and random distribution of the pores.

The microstructural evolution of a material with increasing porosity is a 3D connectivity problem. According to the percolation theory [40], there may exist two critical porosity levels. When the porosity reaches the first critical value (p_{c1}), a microstructural transition occurs from fully isolated and closed pores with nearly spherical or ellipsoidal shapes to open and interconnected with complex shapes. Finally, the effective strength or elastic modulus vanishes when the porosity reaches the second critical value (p_c). For polycrystalline materials composed of identical spherical particles arranged in cubic, orthorhombic and rhombohedral arrays, Knudsen [24] obtained the theoretical p_c values of 0.476, 0.397 and 0.26, respectively. For powder materials, the p_c value seems to be the apparent porosity of the powder before densification by sintering or hot pressing [41]. Therefore, three regimes can be identified: (1) At low porosity levels ($p < p_{c1}$), pores are fully isolated and closed with nearly spherical or ellipsoidal shapes; (2) At intermediate porosity levels ($p_{c1} \leq p < p_c$), interconnected pores with complex shapes are present; (3) The stress-supporting solid framework fails when $p \geq p_c$.

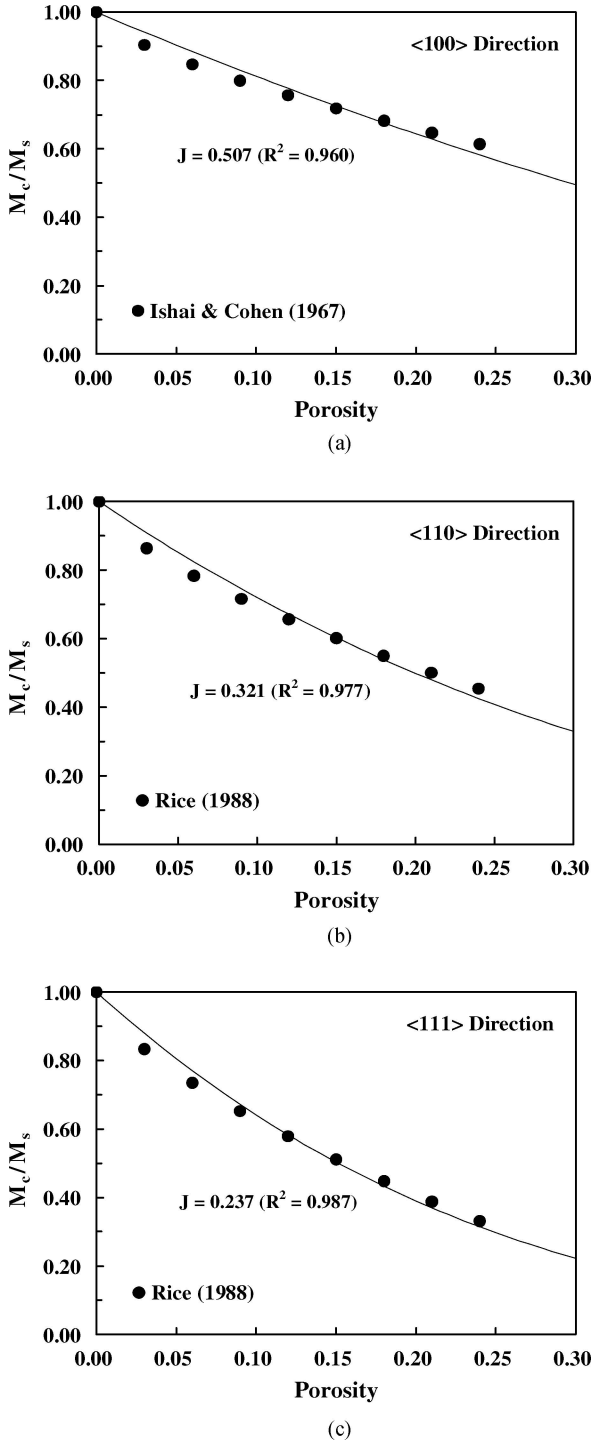

Figure 4 Relative mechanical properties of solids containing cubic pores with their ⟨100⟩ (a), ⟨110⟩ (b) and ⟨111⟩ (c) directions parallel to the loading direction.

One important consequence of the microstructural transition at p_{c1} is that the mechanical properties of porous materials in regime 2 ($p_{c1} \leq p < p_c$) cannot be represented by Equation 4; if this is attempted then there will be an apparent decrease in J with increasing p. Thus, p in Equation 4 for the intermediate regime may be replaced reasonably by the effective porosity (p/p_c) due to the interconnection of pores.

$$\frac{M_c}{M_s} = \left(1 - \frac{p}{p_c}\right)^{1/J} \tag{22}$$

with $p \leq p_c$ and $p_c \leq 1$. Equation 22 yields the same formula proposed by Phani [20] as an empirical equation for the Young's modulus-porosity relation in gypsum systems.

4. Comparison with experiments

Fig. 5 gives an example for the comparison between the experimentally measured relative Young's moduli (E_c/E_s) and the theoretical values calculated from the GMR. The experimental data for porous Al_2O_3 polycrystalline aggregates with porosities ≤30% [42] can be well fitted with Equation 22 with $J = 0.284$ and $p_c = 1$ (Fig. 5a). As shown in Fig. 5b, Equation 22 with $J = 0.263$ and $p_c = 1$ yields a good fit to experimental data for porous Al_2O_3 with $p \leq 40\%$ [27]. Experimental data for porous MgO aggregates with $p \leq 40\%$ [44] are in good agreement with Equation 22 using $J = 0.241$ and $p_c = 1$ (Fig. 5c). Equation 21 with $J = 0.270$ and $p_c = 1$ works very well for fitting the experimental data for polycrystalline SiC aggregates with $p \leq 42\%$ (Fig. 5d, [44]). Porter et al. [45] studied the elasticity of polycrystalline spinel ($MgAl_2O_4$) aggregates prepared by hot pressing. Their data on the porosity-dependence of Young's and shear moduli are consistent with the GMR with $J = 0.270$ (Fig. 5e) and $J = 0.280$ (Fig. 5f), respectively.

Walsh *et al*. [46] carried out a series of experiments on the bulk moduli (K) of glass foams over a range of porosities from 0 to 0.7. In the samples, the pores are nearly spherical and non-interconnecting [47]. Their experimental data are plotted in Fig. 6a for comparison with the values calculated from Equation 22. The experimental data essentially track the calculated curve with $J = 0.505$ and $p_c = 1$ for samples with $p \leq 0.50$. The Hashin-Shtrikman [47] upper bound (HS^+) overestimates the actual elastic modulus. The Hashin-Shtrikman lower bound (HS^-) is physical meaningless because it results in a zero value for all elastic moduli regardless of the porosity. Fig. 6a displays that the GMR yields a better description than the self-consistent (SC, [3, 48, 49]) approximation and the differential method (DM, [49, 50]). Further, the exponential expression Equation 11 is obviously disqualified for describing the data at high porosities.

Ishai and Cohen [51] measured the compressive yield strengths of porous epoxy at constant strain rates from 2.25×10^{-2}/s to 4.50×10^{-5} /s. The samples, containing up to 66% porosities, were prepared by whipping the epoxy liquid at different speeds and times according to the desired void ratios. Most of the pores had nearly spherical geometry. Their experimental data except one (Fig. 6b) are in good agreement with Equation 22 with $J = 0.513$ and $p_c = 1$. The anomaly for a sample with 7%

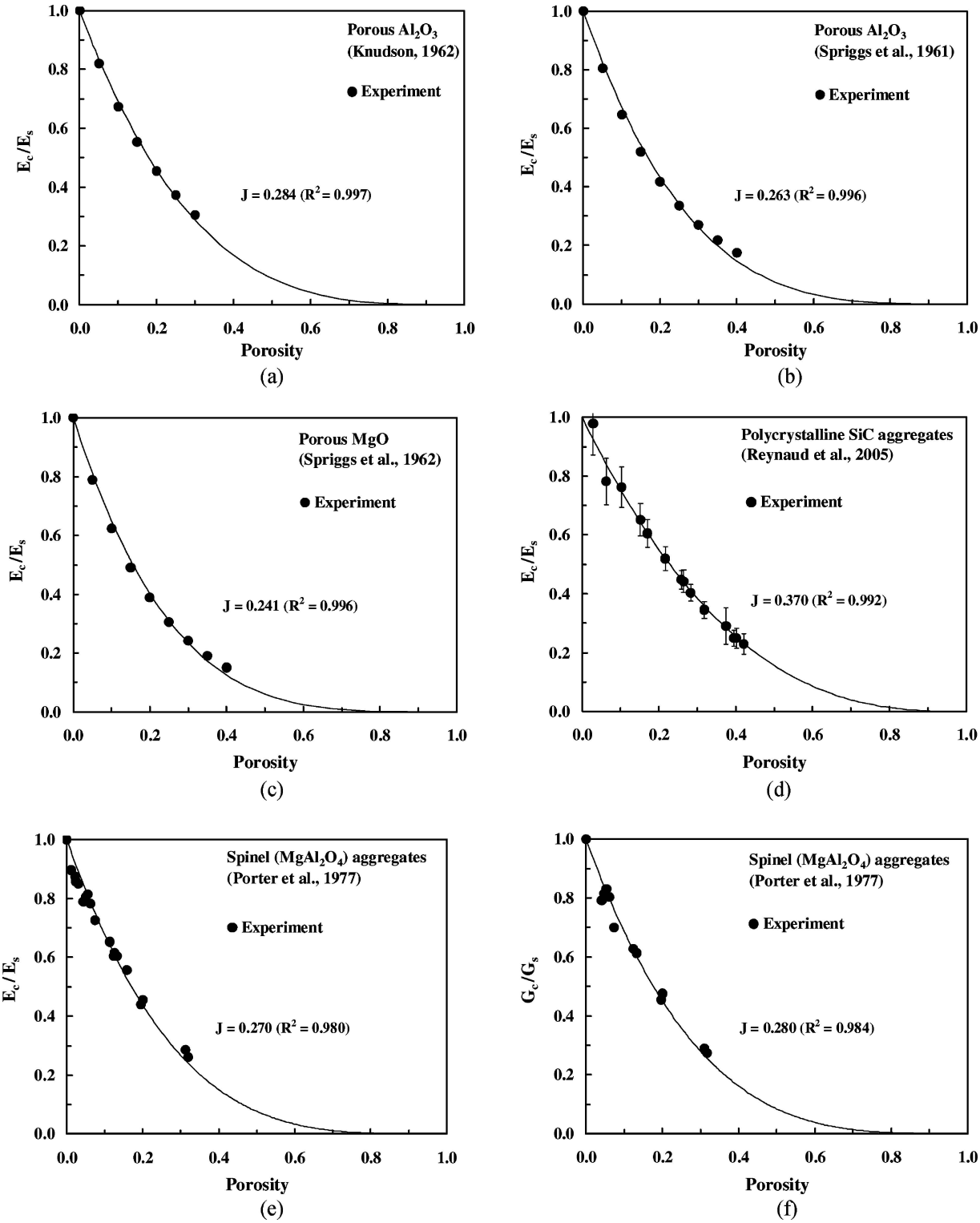

Figure 5 Comparison of the theoretical values calculated from the GMR with experimental data on relative Young's modulus (a–e) and shear modulus (d) of porous materials. (a–b) Al_2O_3 [42, 43], (c) MgO [43], (d) SiC [44], and (e–f) $MgAl_2O_4$ [45].

porosity may be due to some errors in the measurement. For phosphate-bonded, alumina filled, magnesia ceramics dominated by shaped-cornered holes and flat elliptical cavities [52], however, the experimental data (Fig. 6c) are well fitted by the GMR with $J = 0.146$, $p_c = 1$. The experimental data on the compressive strength of Cu/Cu_2O cermets with morphologically complex intergranular pores [53] yield a low value of J ($J = 0.140$, Fig. 6d).

Interestingly, Fig. 6 displays a clear effect of pore geometry on the mechanical properties of solid materials. Isolated spherical pores cause the J value to be higher than shaped-cornered holes and flat elliptical cavities. The

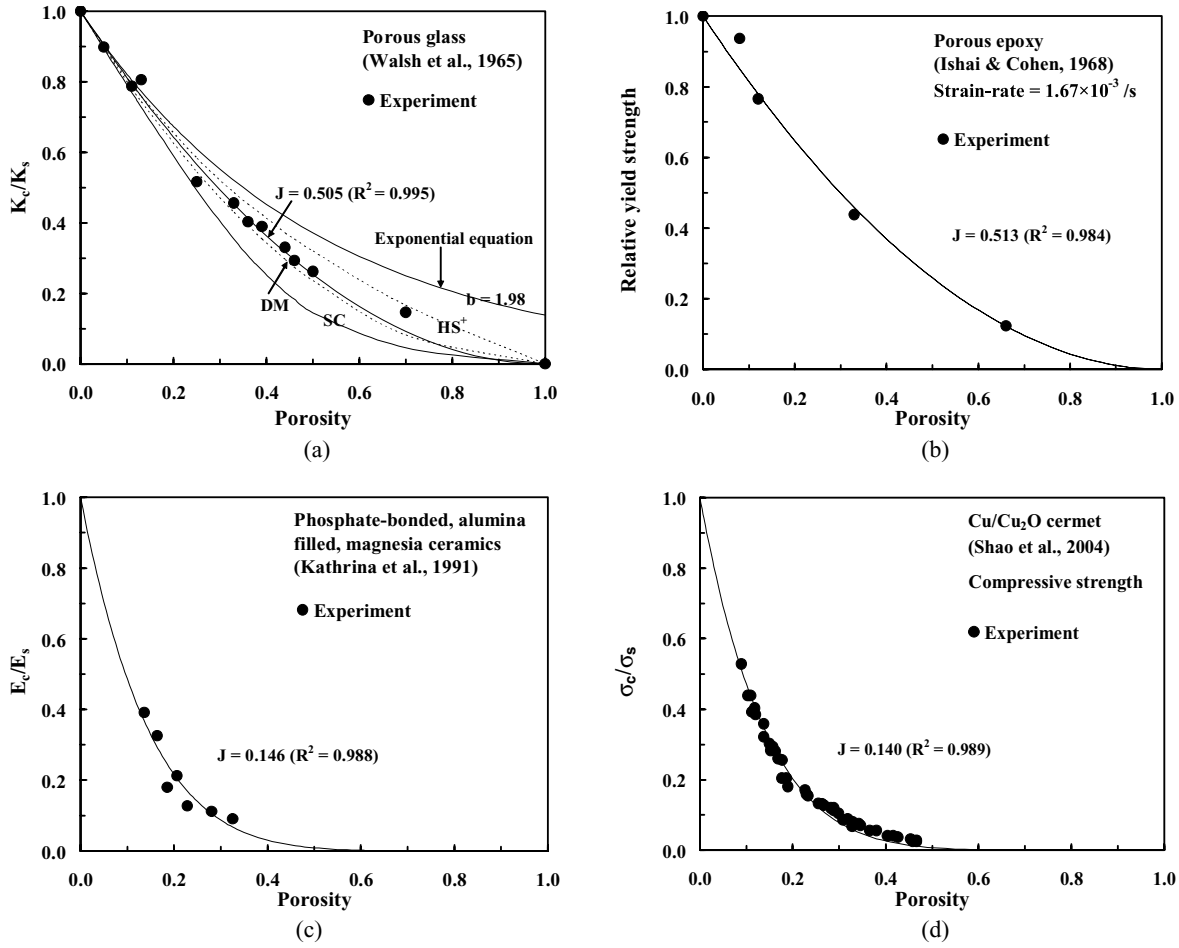

Figure 6 Comparison between experimental and theoretical results for relative bulk modulus for (a) glass foams [44], yield strength of (b) porous epoxy [51], Young's modulus of (c) phosphate-bonded, alumina filled magnesia ceramics [52], and (d) Cu/Cu_2O cermets [53]. DM, HS^+, and SC represent differential method [49, 50], the Hashin-Shtrikman upper bound [47], and the self-consistent approximation [49, 50], respectively.

value of $J \approx 0.5$ for porous glass [47] and epoxy [51] is consistent with the theoretical prediction [21] for a solid containing isolated spherical pores.

The above comparison between calculation and experiment yields consistently $p_c = 1$. This indicates that the effective mechanical properties does not vanish unless $p = 1$. This is also consistent with a fact that it is possible to fabricate ceramics with a porosity as high as 0.93 [13]. This implies that the solid medium in the samples form a continuous stress-supporting framework although the pores can be interconnected. Therefore, Equation 22 is exactly identical to Equation 4, the latter is derived directly from the GMR, for the materials with $p_c = 1$.

Berge *et al*. [54] investigated the elasticity of synthetic sandstone using sintered glass beads with porosities ranging from 1 to 43%. The glass has $E_s = 72.33$ GPa, $G_s = 29.2$ GPa. Fig. 7 displays a clear drop of the relative elastic moduli E_c/E_s and G_c/G_s and towards a critical porosity (p_{c1}) of ~0.30. For porosities below ~0.30, the samples have similar microstructures with isolated pores embedded in a continuous solid glass [54] and the experimental data can be well described by the GMR Equation 4 with $J = 0.405$ and $J = 0.409$ for E and G, respectively. The critical porosity p_{c1} presumably coincides with the minimum porosity for near-closely packed quasi-identical spheres. The J values for E and G decreases progressively from ~0.41 to ~0.25 with increasing porosity from ~0.30 to 0.43, reflecting that the geometry of pores in the synthetic sandstone becomes complex due to the interaction between pores in this range of porosities.

Figs 8 and 9 demonstrate the relationship between ductile strength and porosity for sintered powder metal compacts such iron, cooper, aluminum, nickel and their alloys [10, 55–57]. Up to a porosity $p = \sim 0.25$, the strength of samples can be well described by the GMR Equation 4 with $J = \sim 0.25$. For higher porosities ($p > \sim 0.25$), however, the J value to fit the experimental data decreases progressively with increasing porosity. Although no detailed information about the actual pore shape at different porosity levels is available from the original literature, it is likely that the loss of isolation of the pores occurs at $p > \sim 0.25$. The pores change from being isolated, closed and sharp-cornered to interconnected channel pores.

Using an ultrasonic technique, Matikas *et al*. [58] measured the longitudinal (P-wave) and shear (S-wave)

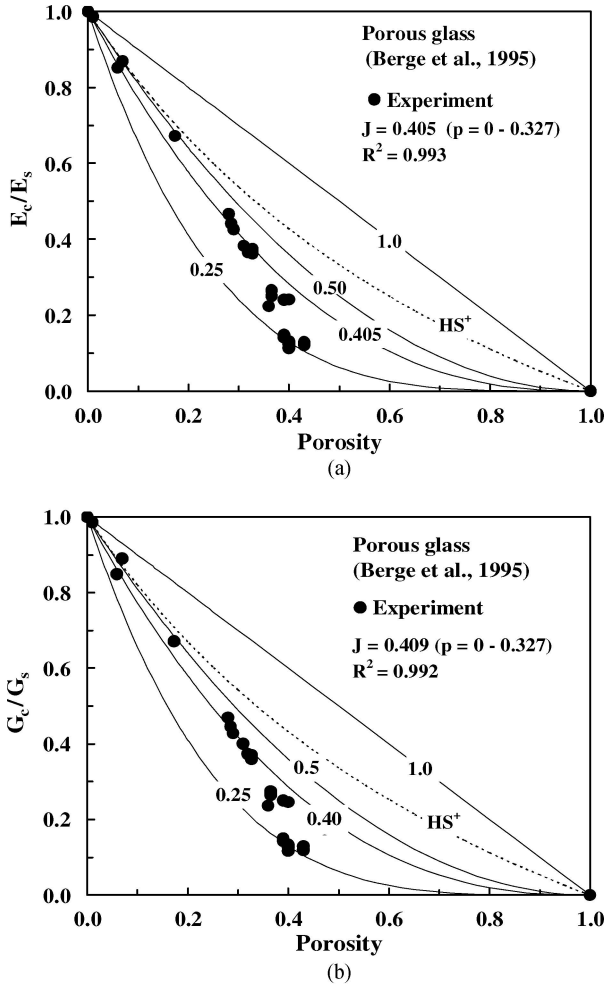

Figure 7 Comparison between experimental and theoretical results for relative Young's modulus (a) and shear modulus (b) for sandstone analogs made from fused glass beads [44]. Theoretical curves labelled according to J values. HS^+ represent the Hashin-Shtrikman upper bound.

acoustic velocities (V_p and V_s) and then calculated the Young's, shear and bulk moduli as well as the Poisson's ratio for porous titanium aluminide compacts. The relative elastic properties as a function of porosity are plotted in Fig. 10. $J = 0.531$ and $J = 0.385$ for V_p and V_s, respectively. For the same set of samples, J values needed to best fit the experimental data are different for different elastic properties: $J = 0.550$, 0.248, 0.227 and 0.134 for the Poisson's ratio (υ), shear modulus (G), Young's modulus (E) and bulk modulus (K), respectively. This aspect should receive a further detailed study.

Fig. 11 illustrates a general trend of the variation in the P- and S-wave velocities in water-saturated basalts at a confining pressure of 200 MPa [59]. The results are of geological interests because the oceanic crust is compositionally dominated by the basalts. The GMR with $J = 0.235$ and $J = 0.214$ provides statistically meaningful descriptions for the V_p and V_s data, respectively. Scatter in the velocity data plots can be attributed to variations in shape, size, and spatial distributions and orientations of pores within the natural basaltic samples.

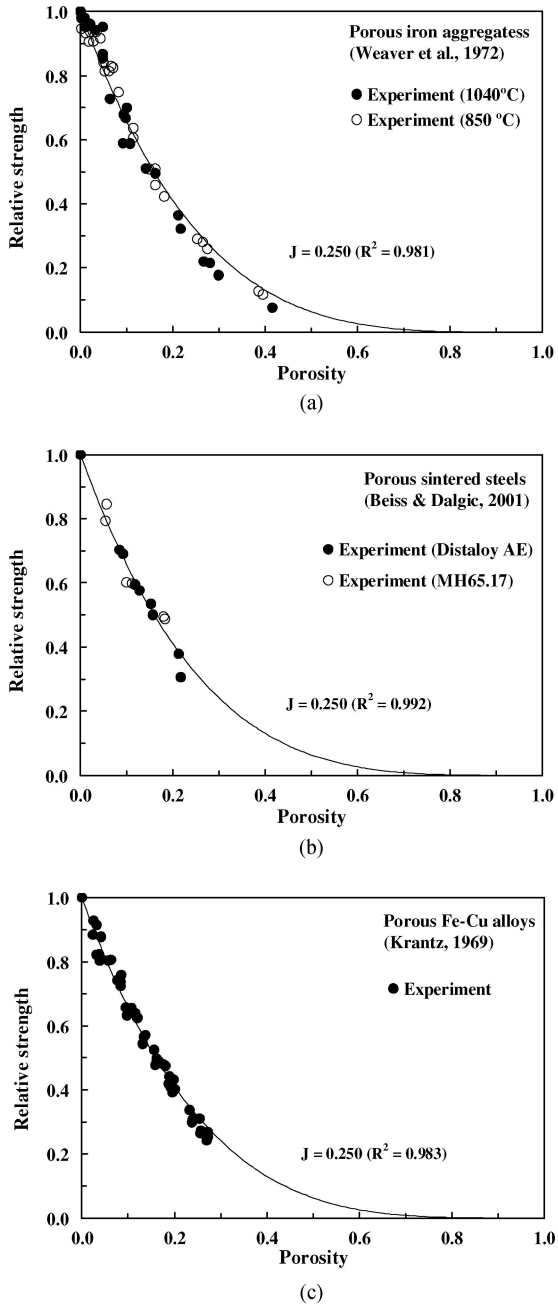

Figure 8 Relative strengths for (a) Fe aggregates [55], (b) sintered steels [10], and (c) Fe-Cu alloys [56] alloys plotted against porosity.

5. Discussion and conclusions

The expression of the generalized mixture rule (GMR) has several characteristics:

(1) The GMR is a rigorous mathematical formula that is of a simple symmetry. It postulates no assumptions on either physical properties or processes (e.g., isostrain or isostress) or microstructures (e.g., oversimplified unit cell). Thus, it is reasonable to believe that the GMR reflects the random nature of microstructure in polyphase materials.

(2) The GMR provides a unified description for the best fitting relationship between the overall mechanical

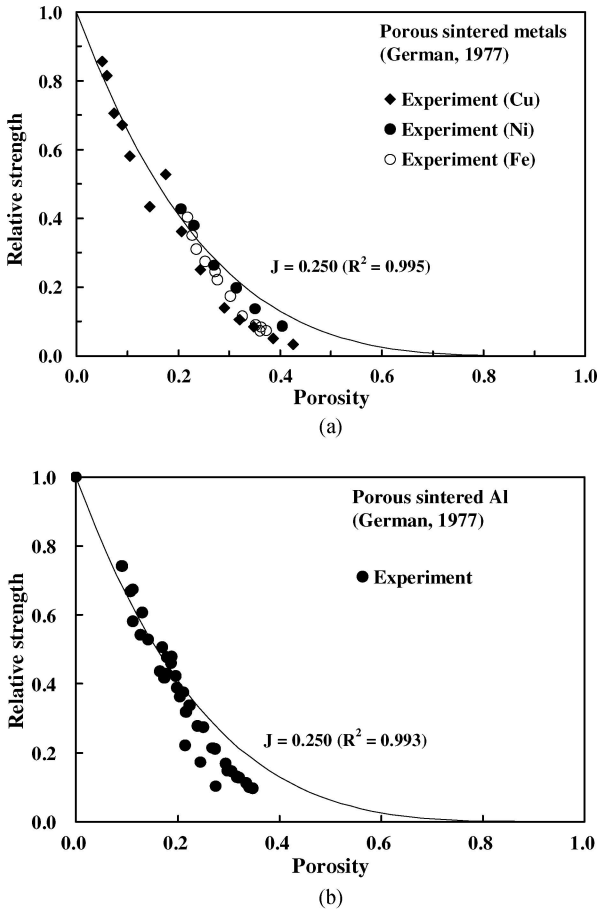

Figure 9 Relative strengths for (a) sintered Cu, Ni and Fe [57] and (b) sintered Al [57] plotted against porosity.

properties (e.g., elastic constants, yield and flow strengths) and the volume fraction and microstructure of each component in the multiphase composites. For porous solids, various well-known equations such as Balshin power law [15], Duckworth exponential equation [26], Gibson-Ashby formula [13], and Phani expression [20] on the relationship between the mechanical properties and porosity can be derived directly from the GMR. For porosities <30%, the GMR is consistent with the results of previous theoretical models based on some idealized uniform structures (e.g., Eudier [11], Ramakrishnan and Arunachalam [38], Ishai and Cohen [39], and Rice [14]) within an error of no more than a few percent. Further, the agreement between the GMR and extensive experimental data on wide ranges of polyphase systems including porous solids could not be considered to be fortuitous. The GMR should have some physical validity as a theory or at least a hypothesis or a phenomenological tool for a general description of the mechanical properties of multiphase materials including porous solids. Rigorous theoretical analyses, which could be a very challenging topic of mathematic mechanics, are definitively needed because the fundamental physical meaning of the GMR has not been clear. Thus the present work provides a foundation upon which to base further studies.

(3) The characteristic exponent J of the GMR provides a scaling parameter for quantitatively describing the effects of complex microstructures on the overall physical properties. This parameter, which is named as the microstructural coefficient, is controlled mainly by the shape, size distribution, continuity and connectivity of the phases, and may reflect the formation processes of the materials. Thus, the J value can be used to classify the polyphase materials. For lotus-type porous materials with long cylindrical or hexagonal pores oriented parallel and perpendicular to the stress direction, $J = 1$ and $J = 1/3$, respectively (Fig. 1). $J \to 0$ (the geometrical mean), which equivalent to the Hashin and Shtrikman lower bound [33] in the case of porous materials), represents an extreme case where the effective property of a porous material will vanish, regardless of porosity. $J = \sim 0.50$ for porous materials in which isolate, perfectly spherical pores are embedded randomly in a continuous solid matrix (Fig. 6a and b). For the Young's modulus, $J = \sim 0.25$ for polycrystalline materials containing shaped-cornered holes (Fig. 2a,

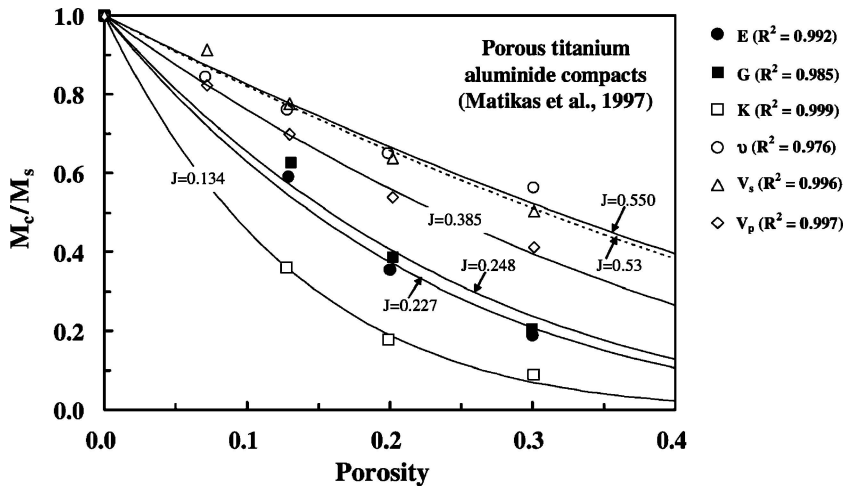

Figure 10 Relative elastic properties (E, G, K, υ, V_p and V_s) for titanium aluminide (Ti-24Al-11Nb) compacts [58] plotted against porosity.

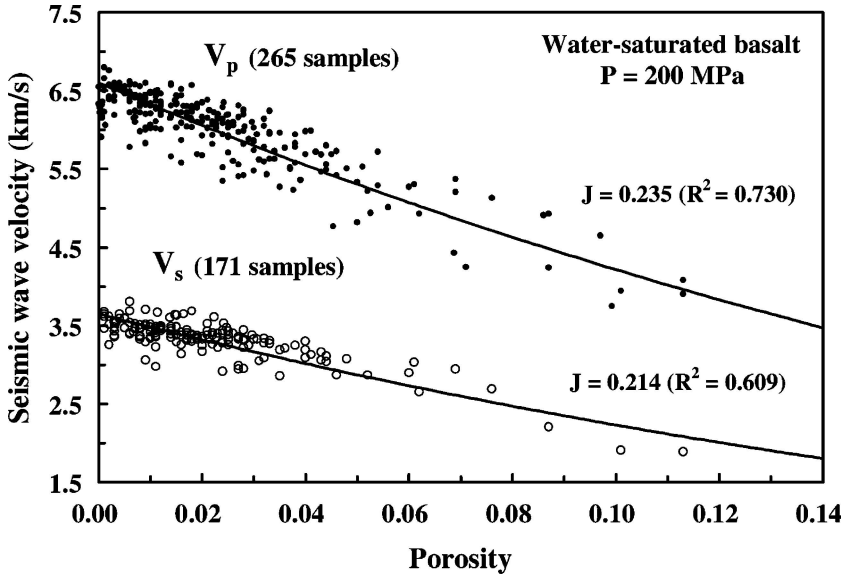

Figure 11 P- and S-wave velocities (km/s) in water-saturated basalts [59] plotted against porosity.

5b and c, 8a–c and 9). The presence of flat elliptical cavities will result in a smaller value of J (Fig. 6c and d). Generally, intergranular, continuous, channel pores cavities cause a lower J value than intragranular, isolated and rounded pores. Hence, rounding and disconnecting the pores should result in an increase in the effective mechanical properties of materials with a constant porosity. In other words, optimizing the overall mechanical properties of materials can be done through introducing different volume fractions and/or different shapes of pores into the solids. An additional finding is that the values of J for shear, Young's, shear and bulk moduli and Poisson's ratio may not be identical even for a porous material with a constant microstructure (Fig. 10). Hence, there is a need for further careful investigation on this subject.

(4) The application of the GMR to predict the overall properties of polyphase materials is more direct compared with other approaches such as Hashin and Shtrikman upper and lower bounds [33]. In the case of elasticity, the GMR does not need to know bulk or shear moduli separately. However, the calculations of Hashin and Shtrikman bounds require full information on the bulk and shear moduli of each phase of the materials. A full set of elastic data is usually lacking because only one elastic property is often measured. In the latter cases, the Hashin and Shtrikman bounds cannot be calculated. For porous materials, the Hashin and Shtrikman upper and lower bounds lie too far apart to be useful in predicting elastic properties as a function of porosity because the pores have a null strength and the Hashin and Shtrikman lower bound is always zero for all moduli regardless of the porosity.

Acknowledgments

Ji thanks the NSERC of Canada and Laboratory of Marginal Sea Geology, Guangzhou Institute of Geochemistry, Chinese Academy of Sciences (Chinese Academy of Sciences, KZCX2-SW-117) for research grants.

References

1. S. JI, *Mater. Sci. Eng.* **A366** (2004) 195.
2. *Idem., J. Geophyis. Res.* **109** (2004) DOI: 10.1029/2004JB003124.
3. R. HILL, *J. Mech. Phys. Solids* **13** (1965) 213.
4. A. E. EINSTEIN, *Ann. Phys. Lpz.* **19** (1906) 289.
5. R. BR. ROSCOE, *J. Appl. Phys.* **3** (1952) 367.
6. S. K. HYUN, K. MURAKAMI and H. NAKAJIMA, *Mater. Sci. Eng.* **A299** (2001) 241.
7. T. ICHITSUBO, M. TANE, H. OGI, M. HIRAO, T. IKEDA and H. NAKAJIMA, *Acta Mater.* **50** (2002) 4105.
8. J. C. RUSS, "Practical Stereology" (Plenum Press, New York, 1986).
9. L. F. NIELSEN, *Mater. Sci. Eng.* **52** (1982) 39.
10. P. BEISS and M. DALGIC, *Mater. Chem. Phys.* **67** (2001) 37.
11. M. EUDIER, *Power Metal.* **9** (1962) 278.
12. B. PAUL, *Trans. Meta. Soc. AIME* **218** (1960) 36.
13. L. J. GIBSON and M. F. ASHBY, "Cellular Solids: Structure & Properties" (Pergamon, Oxford, 1988).
14. R. W. RICE, "Porosity of Ceramics" (Marcel Dekker Inc., New York, 1998).
15. M. Y. BALSHIN, *Akad. Sci. USSR* **67** (1949) 831.
16. P. WONG, J. KOPLIK and J. P. TOMANIC, *Phys. Rev.* **B30** (1984) 6606.
17. A. S. WAGH, R. B. POEPPEL and J. P. SINGH, *J. Mater. Sci.* **26** (1991) 3862.
18. R. HAYNES, *Powder Metall.* **14** (1971) 64.
19. T. J. GRIFFITHS, R. DAVIES and M. B. BASSETT, *ibid.* **3** (1979) 119.
20. K. K. PHANI, *Am. Ceram. Soc. Bull.* **65** (1986) 1584.
21. A. R. BOCCACINI, G. ONDRACEK and E. MOMBELLO, *Mater. Sci. Lett.* **14** (1995) 534.
22. K. S. BLANKS, A. KRISTOFFERSSON, E. CARLSTROM and W. J. CLEGG, *J. Europ. Ceram. Soc.* **18** (1998) 1945.
23. R. W. RICE, *J. Mater. Sci.* **32** (1997) 4731.
24. F. P. KNUDSEN, *J. Am. Ceram. Soc.* **42** (1959) 376.
25. R. W. RICE, "Treatise on Materials Science and Technology. Properties and Microstructures" Vol. 11 (Academic Press, New York, 1977) p. 199.
26. W. H. DUCKWORTH, *J. Am. Ceram. Soc.* **34** (1951) 1.
27. R. M. SPRIGGS, *J. Ceram. Soc.* **44** (1961) 628.

28. N. RAMAKRISHNAN and V. S. ARUNACHALAM, *J. Am. Ceram. Soc.* **76** (1993) 2745.
29. R. MCLAUGHLIN, *Int. J. Eng. Sci.* **15** (1977) 237.
30. A. N. NORRIS, *Mech. Mater.* **4** (1985) 1.
31. W. ZIMMERMAN, *ibid.* **12** (1991) 17.
32. D. P. HASSELMAN, *J. Am. Ceram. Soc.* **45** (1962) 452.
33. Z. HASHIN, *Ceram. Microstr.* **14** (1968) 313.
34. R.ROSSI, *J. Am. Ceram. Soc.* **51** (1968) 433.
35. J. M. LEDERMAN, *J. Appl. Polymer Sci.* **15** (1971) 693.
36. A. N. GENT and A. G. THOMAS, *J. Appl. Polymer Sci.* **1** (1959) 107.
37. L. J. GIBSON and M. F. ASHBY, *Proc. R. Soc. Lond.* **A382** (1982) 43.
38. N. RAMAKRISHNAN and S. ARUNACHALAM, *J. Mater. Sci.* **25** (1990) 3930.
39. O. ISHAI and L. J. COHEN, *Int. J. Mech. Sci.* **9** (1967) 539.
40. D. STAUFFER and A. AHARONY, "Introduction to Percolation Theory" (Taylor and Francis, London, 1992).
41. J. KOVACIK, *J. Mater. Sci. Lett.* **18** (1999) 1007.
42. F. P. KNUDSEN, *J. Am. Ceram. Soc.* **45** (1962) 94.
43. R. M. SPRIGGS, *ibid.* **45** (1962) 454.
44. C. REYNAUD, F. THEVENOT, T. CHARTIER and J. L. BESSON, *J. Eur. Ceram. Soc.* **25** (2005) in press.
45. D. F. PORTER, J. S. REED and D. LEWIS III, *J. Am. Cer. Soc.* **60** (1977) 345.
46. J. B. WALSH, W. F. BRACE and A. W. ENGLAND, *ibid.* **48** (1965) 605.
47. Z. HASHIN and S. SHTRIKMAN, *J. Mech. Phys. Solids* **11** (1963) 127.
48. B. BUDIANSKY, *J. Mech. Phys. Solids* **13** (1965) 223.
49. J. G. BERRYMAN, *J. Energy Resour. Tech.* **116** (1994) 87.
50. M. P. CLEARY, I. W. CHEN and S. M. LEE, *J. Eng. Mech.* **106** (1980) 861.
51. O. ISHAI and L. J. COHEN, *J. Comp. Mater.* **2** (1968) 302.
52. T. KATHRINA, R. ROUND and B. BRIDGE, *J. Phys. D: Appl. Phys.* **24** (1991) 1673.
53. W. Z. SHAO, V. V. IVANOV, L. ZHEN, Y. S. CUI and D. Z. YANG, *J. Mater. Sci.* **39** (2004) 731.
54. P. A. BERGE, B. P. BONNER and J. G. BERRYMAN, *Geophysics* **60** (1995) 108.
55. C. H. WEAVER, R. G. BUTTERS and J. A. LUND, *Inter. J. Powder Metall.* **8** (1972) 3.
56. T. KRANTZ, *Int. J. Powder Metall.* **5** (1969) 35.
57. R. M. GERMAN, *Inter. J. Powder Metall. Tech.* **13** (1977) 259.
58. T. E. MATIKAS, P. KARPUR and S. SHAMASUNDAR, *J. Mater. Sci.* **32** (1997) 1099.
59. S. JI, Q. WANG and B. XIA, "Handbook of Seismic Properties of Minerals, Rocks and Ores" (Polytechnic International Press, Montreal, 2002).

Received 24 February
and accepted 7 June 2005